Pyroelectric camera modulation transfer function

Valentin G. Kolobrodov, MEMBER SPIE
Vita V. Rybalka, MEMBER SPIE
Kiev Polytechnic Institute
Optical System Department
Pobedy pr., 37
Kiev, Ukraine, 252057

Abstract. Real modulation transfer function is developed for a chopper operating pyroelectric camera. Constructive parameter influence on output signal is analyzed.

Subject terms: pyrocameras; pyrovidicons; optical systems; choppers; test patterns; irradiance time modulation; thermal diffusion; pyroelectric response; modulation transfer function.

Optical Engineering 34(4), 1044–1048 (April 1995).

1 Introduction

Thermal imaging cameras having a pyrovidicon (PV) as IR detectors, i.e., pyrocameras (PCs), are widely adopted because of a number of their merits such as uniform responsivity in a wide spectral range, operating without deep cooling, and forming of a standard TV signal. However, a PV peculiarity to respond only to changes in incident radiation causes certain problems in PC design.

There exist two operating regimes for changing PV target irradiation: panning and modulation. The modulation is preferable because it permits displaying images of static and stationary radiating thermal objects.

The modulation transfer function (MTF) is an important performance that indicates a spatial resolution of the PC and a quality of image contrast transfering. In addition, minimum resolvable temperature difference (MRTD) and minimum detectable temperature difference (MDTD) are determined by the MTF. Thus, development and investigation of a real PC MTF with a chopper, which is the task of this paper, is essential.

2 Pyrocamera Elements MTF

A PC being linear and spatially invariant can be described by MTF_c:

$$\mathrm{MTF}_c(f_x,f_y)=\frac{\int_{-\infty}^{\infty}\int h_c(x,y)\,\exp[-j2\pi(xf_x-yf_y)]\,\mathrm{d}x\,\mathrm{d}y}{\int_{-\infty}^{\infty}\int h_c(x,y)\,\mathrm{d}x\,\mathrm{d}y}\,, \quad (1)$$

where the impulse response of the PC, $h_c(x,y)$, is the luminance distribution in a point source image on the display screen. In the general case, a PC consists of consecutively attended elements, thereby,

$$\mathrm{MTF}_C=\mathrm{MTF}_O\cdot\mathrm{MTF}_{M-\mathrm{PV}}\cdot\mathrm{MTF}_E\cdot\mathrm{MTF}_D\,, \quad (2)$$

where the MTF of the optical system, "modulator-pyrovidicon" system, electronic system (videoamplifier) and display, respectively, are considered. Apparently, each MTF's spatial frequencies would be reduced to a common plane, for example, the PV target plane.

In practice, while using standard TV scanning system and an amplifier with wide bandwidth, we can consider $\mathrm{MTF}_E \approx 1$ and $\mathrm{MTF}_D \approx 1$. Rest functions can be reduced to one dimension along the line scanning direction.[1] To approximate MTF_o the Gauss function is used:

$$\mathrm{MTF}_O(f_x)=\exp(-2\pi^2 r_0^2 f_x^2)\,, \quad (3)$$

where r_0 is the point spread function (PSF) radius for 0.606 $\times$ $\mathrm{PSF}_{\max}$ in x-direction.

3 Real MTF_c Development

To define $\mathrm{MTF}_{M-\mathrm{PV}}$ it is necessary to obtain video-signal current caused by cosine test pattern image with periodic time modulation of the incident radiation at angular frequency $\omega=2\pi f_m$.

If chopper has been set in the image plane, then rectangular time modulation must be considered, as shown in Fig. 1(a). For this case, the MTF was obtained in Ref. 2. At modulation frequency $f_m=25$ Hz, ensuring maximum signal MTF is described by the following expression

$$\mathrm{MTF}^{\mathrm{rect}}_{M-\mathrm{PV}}=\frac{\tanh(\alpha\pi/2)}{(\alpha\pi)/2}\,, \quad (4a)$$

Paper UKR-17 received July 1, 1994; accepted for publication Sep. 2, 1994.

where

$$\alpha=\frac{4\pi^2 k f_x^2}{\omega} , \tag{4b}$$

where k is the thermal diffusivity of the PV target in square meters times inverse seconds.

3.1 *PV Target Irradiance*

However, in real PCs, including only one lens, it is impossible to set a chopper accurately in the image plane. Actually the chopper is placed at certain distance δ_m from PV target [Fig. 2(a)], which causes curving of the rectangular irradiance impulse front [Fig. 1(b)].

In the general case, the variable part of the irradiance is given by

$$E(x,t)=(E_0\cos 2\pi f_x x)[F(t)] , \tag{5}$$

where $E_0\cos 2\pi f_x x$ is a Fourier component of the irradiance spatial distribution on the PV target and $F(t)$ is the modulation function.

With some approximation, we have assumed that $F(t)$ is not changed along the target plane. For simplicity, we shall examine a central part of the target. As follows from Fig. 2(a), the diameter of the central gathering beam in the modulation plane is given by $\delta_m(D_0/f')$, where D_0 is the entrance pupil diameter and f' is the focal length. Thus, for impulse front duration we have

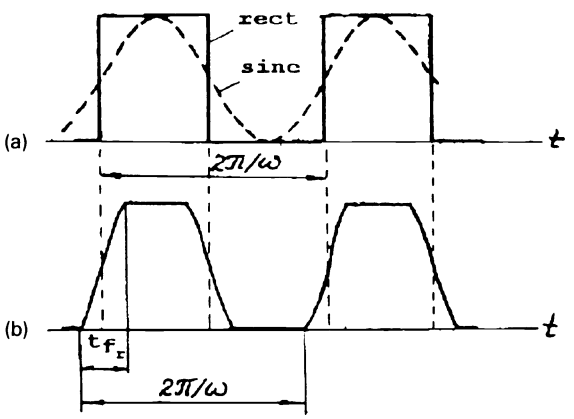

Fig. 1 Diagrams of the target irradiance change with (a) rectangular and sine modulation and (b) real modulation.

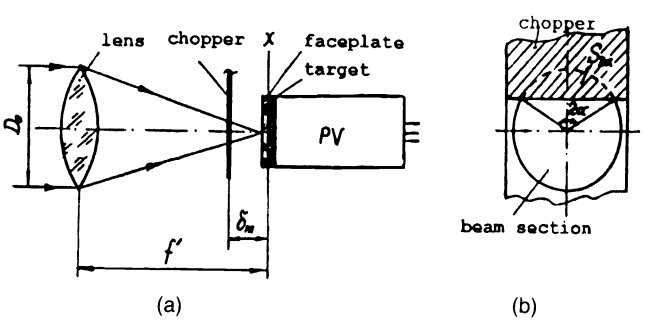

Fig. 2 Scheme of (a) PC chopper setting and (b) the radiation beam shutting.

$$t_{fr}=\frac{\delta_m}{d}\left(\frac{D_0}{f'}\right)t_f , \tag{6}$$

where d is the PV target diameter and t_f is the field duration of a frame scanning.

Referring to Fig. 2(b), showing a chopper, for example, a tape with rectangular windows, performing uniform forward motion and shutting the central beam, we can describe the modulation function for the irradiance impulse front as

$$F_{fr}=\frac{4S_{2\alpha}(t)}{\pi\delta_m^2(D_0/f')^2}=\frac{2}{\pi}$$

$$\times\left\{\arcsin\left(\frac{t}{t_{fr}}\right)^{1/2}-\left(1-\frac{2t}{t_{fr}}\right)\left[\frac{t}{t_{fr}}\left(1-\frac{t}{t_{fr}}\right)\right]^{1/2}\right\} ,$$

$$0<t<t_{fr} . \tag{7}$$

However, for further application, Eq. (7) is not convenient. Therefore $F_{fr}(t)$ has been approximated by sine [Fig. 3(a)]. When $D_0/f'=1$, $d=16$ mm, and δ_m is within the range 2 to 16 mm, the maximum approximation error can be anywhere between 1% and 6.5%, which is suitable.

Thus, irradiance alteration can be expressed by Eq. (5), where modulation function $F(t)$ is defined as

$$F(t)=\begin{cases}\frac{1}{2}\left[1+A\sin\left(\omega t-\frac{1}{2}\omega t_{fr}\right)\right], & \frac{2\pi}{\omega}n<t\le\frac{2\pi}{\omega}n+t_{fr},\\ 1, & \frac{2\pi}{\omega}n+t_{fr}<t\le\frac{\pi}{\omega}(2n+1),\\ \frac{1}{2}\left[1+A\sin\left(\omega t-\frac{1}{2}\omega t_{fr}\right)\right], & \frac{\pi}{\omega}(2n+1)<t\le\frac{\pi}{2}(2n+1)+t_{fr},\\ 0, & \frac{\pi}{\omega}(2n+1)+t_{fr}<t\le\frac{2\pi}{\omega}(n+1),\end{cases} \tag{8}$$

where $A=1/\{\sin[\omega(t_{fr}/2)]\}$.

3.2 *Pyroelectric Response*

It has been assumed that the anisotropic target is uniformly heated through its thickness b. The temperature distribution $T(x,t)$ obeys the thermal balance equation[3]:

$$E_0\cos 2\pi f_x x F(t)+K\left[b\frac{\partial^2 T(x,t)}{\partial x^2}\right]-4\sigma T_0^3-T(x,t)=$$

$$C\left[b\frac{\partial T(x,t)}{\partial t}\right] , \tag{9}$$

where $T(x,t)=T_a(x,t)-T_0$ is the temperature difference between absolute $T_a(x,t)$ and average T_0 temperatures; K is thermal conductivity in $\mathrm{W\,m^{-1}\,deg\,K^{-1}}$; C is volume thermal capacity in $\mathrm{J\,K\,m^{-3}\,deg\,K^{-1}}$; $4\sigma T_0^3$ is radiation conductance, $\mathrm{Wm^{-2}\,deg\,K}$; and σ is the Stephan-Boltzmann constant.

Assuming a harmonic modulation, i.e., $F(t)=e^{j\omega t}$, Eq. (9) has the solution

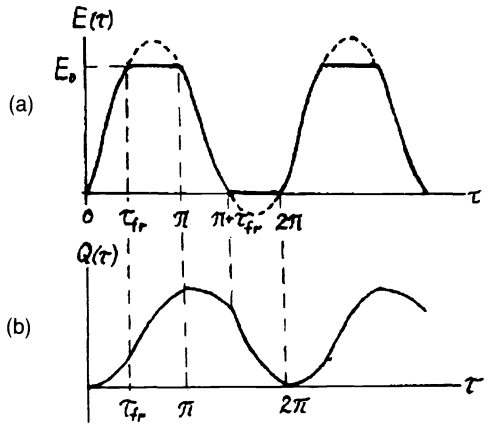

Fig. 3 Diagrams of (a) real irradiance change and (b) pyroelectric charge change.

$$T(x,t)=\frac{E_0}{Kb}\cos 2\pi f_x x e^{j\omega t}\left[(2\pi f_x)^2+\frac{j\omega}{k}\right]^{-1}, \tag{10}$$

where parameter α is defined by Eq. (4a). This solution, Eq. (10), coincides with the approximation of the accurate solution of the 2-D thermal conduction equation, given in Ref. 4.

To obtain the solution of Eq. (9) with the real modulation according to Eq. (8), we can use a general superposition principle.

Modulation function $F(t)$ can be written as the convolution with $(2\pi)/\omega$ periodic sequence of Dirac delta functions:

$$F(t)=\sum_{m=-\infty}^{\infty}\int_0^{2\pi/\omega}\delta\left(t-t_0-\frac{2\pi m}{\omega}\right)F(t_0)\,dt_0$$

$$=\int_0^{2\pi/\omega}F(t_0)\sum_{m=-\infty}^{\infty}\delta\left(t-t_0-\frac{2\pi m}{\omega}\right)dt_0$$

$$=\int_0^{2\pi/\omega}F(t_0)\sum_{n=-\infty}^{\infty}\frac{\omega}{2\pi}\exp[jn\omega(t-t_0)]\,dt_0\ . \tag{11}$$

Applying Eq. (10) to each Fourier component from Eq. (11), we have defined temperature response corresponding to input δ functions periodic sequence:

$$T^{\delta}=\frac{E_0}{Kb}\cos 2\pi f_x x\sum_{n=-\infty}^{\infty}\frac{\omega}{\pi}\times\left[(2\pi f_x)^2+\frac{jn\omega}{k}\right]^{-1}\exp[jn\omega(t-t_0)]\ . \tag{12}$$

The surface density of a pyroelectric charge caused by temperature distribution $T(x,t)$ is given by

$$Q(x,t)=pT(x,t)\ , \tag{13}$$

where p is the pyroelectric coefficient in Cl m^{-2} deg K^{-1}.

By denoting dimensionless time $\tau=\omega t$ and using the calculated sum from Eq. (12), we have obtained

$$Q^{\delta}(\tau)=\frac{pE_0}{\omega Cb}\cos 2\pi f_x x\left(\frac{\omega_0}{\pi}\right)\frac{\pi}{\sinh\alpha\pi}\exp\{\alpha[\pi-(\tau-\tau_0)]\}\ ,$$

$$0<\tau-\tau_0<2\pi\ . \tag{14}$$

Therefore, the pyroelectric charge with real radiation modulation law is described by

$$Q(\tau)=\int_0^{\tau}Q^{\delta}(\tau-\tau_0)F(\tau_0)\,d\tau_0$$

$$+\int_{\pi}^{2\pi}Q^{\delta}(\tau-\tau_0+2\pi)F(\tau_0)\,d\tau_0\ , \tag{15a}$$

$$F(\tau_0)=\begin{cases}\frac{1}{2}\left[1+A\sin\left(\tau_0-\frac{1}{2}\tau_{fr}\right)\right], & 0<\tau_0\leq\tau_{fr}\ ,\\ 1\ , & \tau_{fr}<\tau_0\leq\pi\ ,\\ \frac{1}{2}\left[1+A\sin\left(\tau_0-\frac{1}{2}\tau_{fr}\right)\right], & \pi<\tau_0\leq\pi+\tau_{fr}\ ,\\ 0\ , & \pi+\tau_{fr}<\tau_0\leq 2\pi\ ,\end{cases} \tag{15b}$$

where $\tau_{fr}=\omega\tau_{fr}$.

If a chopper is opened in a half-period, $0<\tau<\pi$, then a pyroelectric charge is determined differently within intervals $0<\tau<\tau_{fr}$ and $\tau_{fr}<\tau<\pi$ [Fig. 3(b)].

$$Q(\tau)=\frac{pE_0}{Cb}\cos 2\pi f_x x\frac{1}{2\sinh\alpha\pi}\left\{\int_0^{\tau}\left[1+A\sin\left(\tau_0-\frac{1}{2}\tau_{fr}\right)\right]\right.$$

$$\times\exp[\alpha(\tau_0-\tau+\pi)]\,d\tau_0+\int_{\tau}^{\tau_{fr}}\left[1+A\sin\left(\tau_0-\frac{1}{2}\tau_{fr}\right)\right]$$

$$\times\exp[\alpha(\tau_0-\tau-\pi)\,d\tau_0]+2\int_{\tau_{fr}}^{\pi}\exp[\alpha(\tau_0-\tau-\pi)\,d\tau_0$$

$$\left.+\int_{\pi}^{\pi+\tau_{fr}}\left[1+A\sin\left(\tau_0-\frac{1}{2}\tau_{fr}\right)\right]\times\exp[\alpha(\tau_0-\tau-\pi)]\,d\tau_0\right\}\ ,\quad 0<\tau<\tau_{fr}\ , \tag{16a}$$

$$Q(\tau)=\frac{pE_0}{Cb}\cos 2\pi f_x x\frac{1}{2\sinh\alpha\pi}\left\{\int_0^{\tau_{fr}}\left[1+A\sin\left(\tau_0-\frac{1}{2}\tau_{fr}\right)\right]\times\exp[\alpha(\tau_0-\tau+\pi)]\,d\tau_0+2\int_{\tau_{fr}}^{\tau}\times\exp[\alpha(\tau_0-\tau+\pi)]\,d\tau_0+2\int_{\tau}^{\pi}\times\exp[\alpha(\tau_0-\tau-\pi)]\,d\tau_0+\int_{\pi}^{\pi+\tau_{fr}}\left[1+A\sin\left(\tau_0-\frac{1}{2}\tau_{fr}\right)\right]\times\exp[\alpha(\tau_0-\tau-\pi)]\,d\tau_0\right\},\quad \tau_{fr}<\tau<\pi\ . \tag{16b}$$

It can be easily shown that in a half-period a chopper opened to maximum pyroelectric charge change is equal by absolute value to a charge change in a half-period a closed chopper:

$$\Delta Q=Q(\pi)-Q(0)=Q(\pi)-Q(2\pi)=\frac{2pE_0}{Cb}\times\cos 2\pi f_x x\left(\frac{e^{\alpha\pi}-1+e^{\alpha\tau}\tau_{fr}(e^{-\alpha\pi}-1)}{\alpha(e^{\alpha\pi}-e^{-\alpha\pi})}+\frac{(1-e^{-\alpha\pi})\{e^{\alpha}\tau_{fr}\sin[(1/2)\tau_{fr}-\Phi_s]+\sin[(1/2)\tau_{fr}+\Phi_s]\}}{(e^{\alpha\pi}-e^{-\alpha\pi})(1+\alpha^2)(1/2)\sin(\tau_{fr}/2)}\right) \tag{17a}$$

where $\Phi_s=\operatorname{arctg}(1/\alpha)$. (17b)

If at the real modulation frequency given the maximum response,[1] $f_m=(1/2t_f)=25$ Hz, the pyroelectric charge commutation without rest occurs at the end of a modulation half-period, then the video-signal current is given by

$$I=\frac{S}{t_f}\Delta Q\ , \tag{18}$$

where S is the effective PV target surface.

3.3 *Modulator-Pyrovidicon System MTF*

$\mathrm{MTF}_{M-\mathrm{PV}}$ is defined as the normalized ratio of video-signal current, caused by the cosine test pattern image, to the maximum possible current for such an image:

$$\mathrm{MTF}_{M-\mathrm{PV}}=\frac{\exp(-\alpha\pi/2)}{\pi\cosh(\alpha\pi/2)}\left(\frac{1}{\alpha}(e^{\alpha\pi}-e^{\alpha}\tau_{fr})+(1+\alpha^2)^{-1/2}\times\{e^{\alpha}\tau_{fr}\sin[(\tau_{fr}/2)-\phi_s]+\sin(\tau_{fr}/2)+\Phi_s]\}1/\sin(\tau_{fr}/2)\right)\ , \tag{19}$$

where $\tau_{fr}=2\pi f_m t_f(D_0/f')\delta_m/d$.

It follows from a comparison of Eqs. (4a) and (19) that an $\mathrm{MTF}_{M-\mathrm{PV}}$ decrease occurs by modulation law distortion. Hence,

$$\lim_{\alpha\to 0}\frac{\mathrm{MTF}^{\mathrm{real}}_{M-\mathrm{PV}}}{\mathrm{MTF}^{\mathrm{rect}}_{M-\mathrm{PV}}}=\left[1-\frac{\delta_m}{d}\left(\frac{D_0}{f'}\right)\right]\ . \tag{20}$$

For example, at $d=16$ mm, $(D_0/f')=1$ and $\delta_m=2$ mm $\mathrm{MTF}_{M-\mathrm{PV}}$ is decreasing by 12.5% and at $\delta=10$ mm by 62.5%. Although the modulation plane and image plane are superposed, i.e., $t_{fr}\to 0$, $\mathrm{MTF}^{\mathrm{real}}_{M-\mathrm{PV}}\to\mathrm{MTF}^{\mathrm{rect}}_{M-\mathrm{PV}}$, while $t_{fr}\to t_f$, i.e.,

$$\delta_m\to d\left(\frac{D_0}{f'}\right)^{-1}\ ,\quad \mathrm{MTF}^{\mathrm{real}}_{M-\mathrm{PV}}\to\mathrm{MTF}^{\mathrm{sine}}_{M-\mathrm{PV}}\ ,$$

where $\mathrm{MTF}^{\mathrm{sine}}_{M-\mathrm{PV}}=(2/\pi)[\cos\Phi_s/(1+\alpha^2)^{1/2}]$.

The preceding expression is correct only when the target points for modulation and scanning phases are equal. Because $f_x\to 0$, $\Phi_s\to(\pi/2)$, i.e., $\mathrm{MTF}^{\mathrm{sine}}_{M-\mathrm{PV}}\to 0$, hence for performance improvement it is required to introduce a phase shift, $\tau_s=\omega t_s$, which now gives

$$\mathrm{MTF}^{\mathrm{sine}}_{M-\mathrm{PV}}=\frac{2}{\pi}\cos(\omega t_s-\Phi_s)(1+\alpha^2)^{-1/2}\ , \tag{21}$$

where t_s is the time shift between modulation and TV scanning periods.

At $f_m=25$ Hz shift $t_s=(t_f/4)$ gives a considerable improvement of $\mathrm{MTF}^{\mathrm{sine}}_{M-\mathrm{PV}}$, which is shown in Fig. 4. However δ_m increasing to $\delta_m=d(D_0/f')^{-1}$, $\mathrm{MTF}^{\mathrm{real}}_{M-\mathrm{PV}}$, cannot be treated as $\mathrm{MTF}^{\mathrm{sine}}_{M-\mathrm{PV}}$, because in this case, irradiance changes at all target points occur simultaneously. Thereby, the phase shift will differ along the target. For example, for upper and lower PV target lines shift τ_s differs by π. Thus at $f_m=25$ Hz, image contrast inverting will be present along the screen. The $\mathrm{MTF}_{M-\mathrm{PV}}$, calculated for PV with a triglycine sulphate (TGS) target, having $k=3\times10^{-7}$ m^2 s^{-1}. These are plotted in Fig. 4 for different values of δ_m.

Therefore, for a pyroelectric camera with the chopper setting at distance δ_m from PV target, MTF_c is found to be

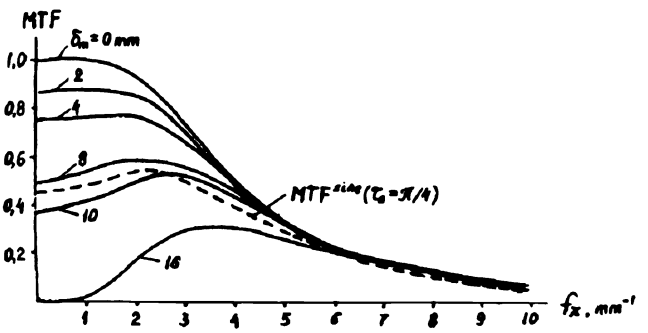

Fig. 4 $\mathrm{MTF}_{M-\mathrm{PV}}$ for different δ_m values.

$$\mathrm{MTF}_c=\frac{1}{\pi}\exp(-2\pi^2 r_0^2 f_x^2)\frac{\exp(-\alpha\pi/2)}{\cosh(\alpha\pi/2)}$$
$$\times\left(\frac{1}{\alpha}\left\{\exp(\alpha\pi)-\exp\left[\alpha\omega t_f\frac{\delta_m}{d}\left(\frac{D_0}{f'}\right)\right]\right\}\right.$$
$$+(1+\alpha^2)^{-1/2}\left\{\exp\left(\alpha\omega t_f\frac{\delta_m}{d}\frac{D_0}{f'}\right)\right.$$
$$\times\sin\left[\frac{\omega t_f}{2}\frac{\delta_m}{d}\left(\frac{D_0}{f'}\right)-\Phi_s\right]+\sin\left[\frac{\omega t_f}{2}\frac{\delta_m}{d}\left(\frac{D_0}{f'}\right)+\Phi_s\right]\left.\right\}$$
$$\left.\times\frac{1}{\sin[(\omega t_f/2)(\delta_m/d)(D_0/f')]}\right). \qquad (22)$$

Figure 5 shows MTF_o of the optical system with lens resolution $v_0=10\ \mathrm{mm}^{-1}$ so that $r_0=1/(2\pi v_0)$. Also in Fig. 5 $\mathrm{MTF}_{M-\mathrm{PV}}$ and MTF_c with the chopper placed at 4-mm distance from lens image plane are plotted.

4 Conclusion

We have investigated a signal transformation process in a PC with a chopper and developed an expression describing a real PC MTF. The analysis of MTF_c, including several components, shows an optical system with negligible influence on MTF_c. The "modulator-PV" system is of the greatest importance in spatial-frequency filtration of the image. This is accounted for by the target temperature spatial distribution as the result of thermal diffusion, which significantly depends on modulation function, determined by modulation system construction.

Thus, chopper setting longitudinal error δ_m, which defines the modulation plane lack of coincidence with the image plane, causes a distortion of the modulated radiation rectangular impulse fronts. At low spatial frequencies, the last involves an output signal that decreases by a quantity that depends on δ_m. At $f_x\to 0$, the signal decreases $[1-(\delta_m/d)(D_0/f')]$ times. If we assume the contrast transfer worsens two times as much, then the maximum permissible δ_m may be equal to 8 mm. While δ_m is increasing, some signal increase appears at spatial frequencies from 1 to 3 mm^{-1} in comparison with lower frequencies (Fig. 4). This is explained by the presence of a sine component in a pyroelectric response, Eq. (17a). This sine part has a phase shift, depending on spatial frequency, relative to modulation function. With

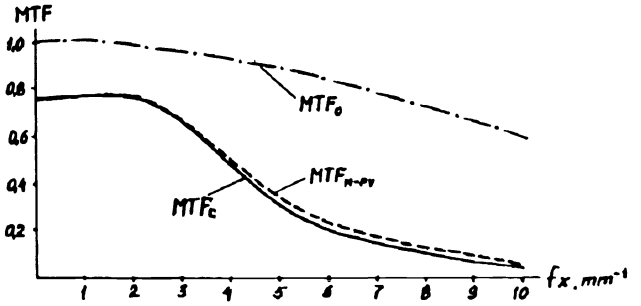

Fig. 5 Real $\mathrm{MTF}_{M-\mathrm{PV}}$, MTF_O and MTF_C.

$\delta_m\to d\,(D_0/f')^{-1}$, the MTF_c will differ across the line scanning direction on the PV target. In addition, contrast inversion will be evident. Thus it becomes impossible to decipher a thermal pattern image.

Therefore, to improve PC image quality it is necessary to put a chopper in an intermediate image plane, which must be realized by the application of new chopper construction and special optical systems.

References

1. J. M. Lloyd, *Thermal Imaging Systems,* Plenum Press, New York (1970).
2. B. Kazan, Ed., *Advances in Image Pickup and Display,* Vol. 3, Academic Press, New York (1975).
3. L. E. Garn, "Fundamental noise limits of thermal detectors," *J. Appl. Phys.* **55**(5), 1243–1253 (1984).
4. R. M. Logan and T. P. McLean, "Analysis of thermal spread in a pyroelectric imaging system," *Infrared Phys.* **3**(7), 15–24 (1973).

Valentin G. Kolobrodov is a professor and heads the Optical Engineering Department of the Kiev Polytechnic Institute. He received an MS in radiophysics from the Kiev State University in 1970 and his PhD in optical devices from the Kiev Polytechnic Institute. His research interests include IR devices and systems, thermovision systems, multispectral radiometric instruments, IR optical systems, metrologic instruments for IR measurement of characteristics of thermovision systems, and IR optical systems. He has 113 publications. He holds or coholds 40 patents. He is a member of the Optical Society of Ukraine and SPIE.

Vita V. Rybalka is a postgraduate student in the Optical Engineering Department of the Kiev Polytechnic Institute. She received her MS in optical devices from the Kiev Polytechnic Institute in 1986. Her thesis was on thermal imaging systems with pyrovidicons. She has four patents related to modulation systems for pyroelectric cameras. She is a member of the Optical society of Ukraine and SPIE.